MAGNETIC RESONANCE IN CHEMISTRY, VOL. 35, 839–844 (1997)

Chelate-Type Intramolecular Hydrogen Bridging in 2,4-Diaryl-6-(2-hydroxy-4-methoxyphenyl)-1,3,5-triazines. A Dynamic $^{1}H/^{13}C$ NMR Study

P. Fischer* and A. Fettig
Institut für Organische Chemie und Isotopenforschung, Universität Stuttgart, Pfaffenwaldring 55, D-70569 Stuttgart, Germany

The energy for breaking the intramolecular hydrogen bond between the phenolic OH and an aza nitrogen in two 2,4-diaryl-6-(2-hydroxy-4-methoxyphenyl)-1,3,5-triazines was determined, by dynamic ^{1}H and ^{13}C NMR spectroscopy, as 55 ± 5 kJ mol^{-1}. The activation parameters $\Delta H^{\ddagger}$ and $\Delta S^{\ddagger}$ for the corresponding internal rotation were derived from a $\Delta G_C^{\ddagger}$–T_C plot. The strength of the chelate-type hydrogen bond is the rationale for the excellent photostabilizing capacity of this class of triazines. It is demonstrated explicitly that the line separation $\Delta\nu$ of the signals under exchange must be extrapolated to the coalescence temperature when $\Delta G_C^{\ddagger}$ values are to be calculated by the Gutowsky–Holm equation. Correct lineshape analysis likewise depends on employing the requisite $\Delta\nu$ value for each temperature. © **1997 John Wiley & Sons, Ltd.**

Magn. Reson. Chem. **35**, 839–844 (1997) No. of Figures: 6 No. of Tables: 1 No. of References: 20

Keywords: NMR; ^{1}H NMR; ^{13}C NMR; 2,4-diaryl-6-(2-hydroxyaryl)-1,3,5-triazines; intramolecular hydrogen bond; dynamic NMR; activation parameters

Received 19 February 1997; revised 2 June 1997; accepted 21 June 1997

INTRODUCTION

Measuring NMR spectra at variable temperature has long been the method of choice for studying molecular kinetics in the 10^{1}–10^{-5} s^{-1} range (dynamic NMR spectroscopy, DNMR).[1,2] The best-documented example is the hindered rotation about the partial C—N double bond in *N*,*N*-dimethylformamide[3–5] and other mono- or dialkylcarboxamides.[6] For the reorientation around this particular partial double bond, the free energy of activation has been determined as 84 kJ mol^{-1} (in acetone-d_6, 113 °C, 1.41 T).[4]

Breaking chelate-type intramolecular hydrogen bonds requires an activation energy of the same order of magnitude. Such strong hydrogen bridging is characteristic, for instance, of a class of new, technically important UV stabilizers, the 2,4-diaryl-6-(1-hydroxyaryl)-1,3,5-triazines (Fig. 1).[7,8] The photostabilizing potential of these compounds relies on the H bond being strong enough in the ground state not to be broken by either polar solvents, e.g. DMSO, or polar functionalities in the polymer in which the stabilizer is embedded.[9] Quantitative data on the strength of the intramolecular hydrogen bond for a specific triazine thus could serve as a first indicator of its intrinsic photostabilizing capacity.

As shown in Fig. 2, fixing the O—H···N bridge between the phenolic hydroxyl function and one of the *ortho*-aza nitrogens in the triazine ring differentiates the 'lower half' of the molecule into a *syn* and an *anti*

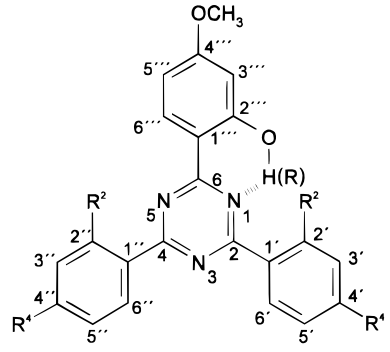

comp.	R	R^2	R^4
1	H	CH_3	CH_3
2	H	OCH_3	OCH_3
3	CH_3	H	CH_3

Figure 1. 2,4-Diaryl-6-(2-hydroxy-4-methoxyphenyl)- and -6-(2,4-dimethoxyphenyl)-1,3,5-triazines **1–3** with the positional numbering used in this paper.

* *Correspondence to:* P. Fischer.

 CCC 0749–1581/97/120839–06 $17.50

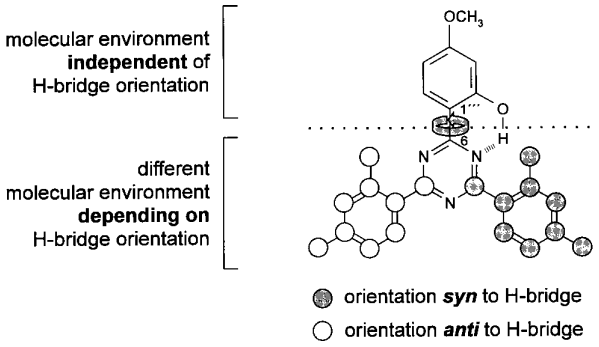

Figure 2. Schematic representation of the chemical exchange process, i.e. breaking the O—H···N hydrogen bridge to N-1 and reforming it to N-5, after rotation of the 6-(2-hydroxy-4-methoxyphenyl) moiety around the C-1‴—C-6 bond.

region. Two sets of molecular environment thus exist for C-2,4 in the triazine, in addition to the two aryl groups at these positions, indicated by empty and shaded circles, respectively, in Fig. 2. Breaking the O—H···N(1) bridge and reforming it to N-5 interchanges the *syn* and *anti* environment for each nuclear position. Hence (2-hydroxyaryl)triazines constitute a perfect example of a two-site exchange process free of additional complications, e.g. by spin–spin coupling.

For a wide range of such triazines, both the ^{1}H and ^{13}C NMR spectra display different stages of coalescence for specific pairs of signals, corresponding to delicately graded activation energies for breaking the intramolecular hydrogen bond in the individual compounds.[10] We have now determined, by temperature-dependent NMR spectroscopy, the activation parameters of this process for two representative members of the series: 2,4-bis(2,4-dimethylphenyl)-6-(2-hydroxy-4-methoxyphenyl)-1,3,5-triazine (**1**), 2,4-bis(2,4-dimethoxyphenyl)-6-(2-hydroxy-4-methoxyphenyl)-1,3,5-triazine (**2**) and 2,4-bis(4-methylphenyl)-6-(2,4-dimethoxyphenyl)-1,3,5-triazine (**3**) (the same order as in **1** and **2** was used for numbering the positions in **3**; see Fig. 1).

Compound **3**, with an *o*-methoxy group in the 6-aryl moiety, cannot form an intramolecular hydrogen bridge and is included as internal reference for monitoring the *intrinsic* temperature dependence of the chemical shifts for individual positions, without the influence of the intramolecular hydrogen bond (see Results and Discussion).

RESULTS AND DISCUSSION

Figure 3 shows, as an example, the partial spectra (measured at 7.04 T) for the *o*-CH_3 protons of the *syn*- and *anti*-2,4-dimethylphenyl ring in **1**. The two singlets, which are well separated at 223 K, appear severely broadened at 273 K. At 277 K, the spectrum still shows two distinct 'humps' which have disappeared, however, at 278 K. The significantly reduced half-height width of the coalesced signal at 279 K clearly indicates that the coalescence point has been surpassed. Figure 3 thus demonstrates the signal form for those nuclear positions, affected by the chemical exchange process, to be sufficiently well differentiated for each 1 K increment. The coalescence temperature might be visually fixed, therefore, to ± 0.5 K. Since temperature measurement is accurate only to ± 1 K, however (see Experimental), closer intervals between the individual NMR traces appear experimentally not sensible.

Table 1 gives the coalescence temperatures for all other positions in **1** which are differentiated by the exchange process. They have been determined at two different field strenghts, 7.04 and 11.74 T, corresponding to 300 and 500 MHz ^{1}H nominal frequency, respec-

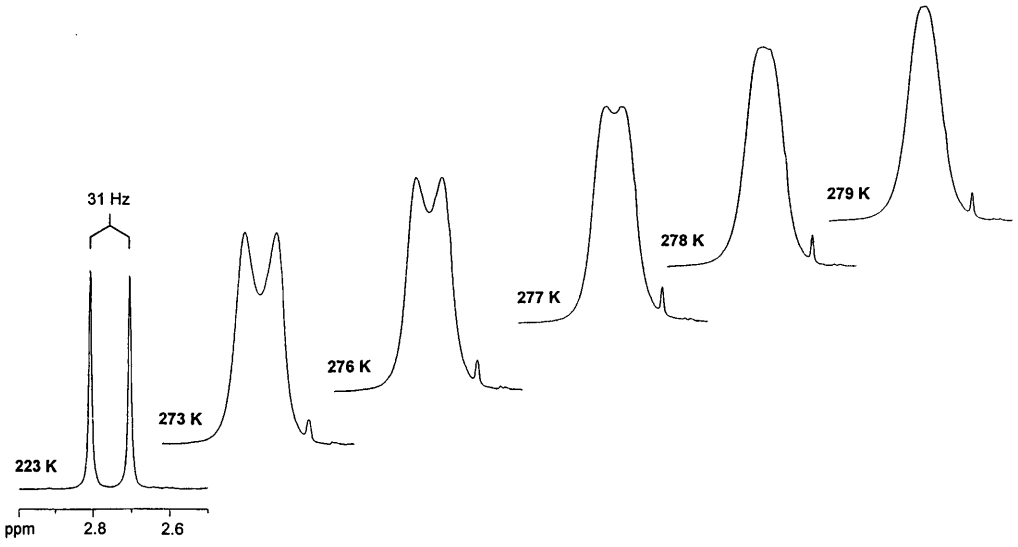

Figure 3. Temperature dependence of the proton NMR signals (7.04 T) for the 2′/2″-methyl groups in compound **1** in the 223–279 K range. Signal amplitudes are not represented to exactly the same scale; especially, the slow-exchange limit lines at 223 K are reduced, for better comparison, by a factor of 5. In the spectra with exchange broadening, a small signal at 2.62 ppm becomes apparent which stems from an impurity (<1%) and is not visible besides the sharp resonance lines of the low-temperature spectrum.

Table 1. Coalescence parameters for the temperature-dependent ^1H and ^{13}C signals in compounds 1 and 2

Compound	Position[a] *syn*	Position[a] *anti*	Field[b]	T_c (K)	$\Delta\nu$ (Hz) At $T \ll T_c$[c]	$\Delta\nu$ (Hz) Extrapolated to T_c[d]	$\Delta G_c^{\ddagger}$ (kJ mol^{-1})
1	2′-CH_3	2″-CH_3	A	278	30.6	33.3	58.0
			B	281	51.3	55.7	57.4
	4′-CH_3	4″-CH_3	B	248	5.8	2.9	56.5
	6′-*H*	6″-*H*	A	289	89.3	96.7	57.8
			B	293	152.3	161.7	57.3
	C-1′	*C*-1″	A	272	23.2	21.2	57.7
			B	274	38.5	34.5	57.0
	C-5′	*C*-5″	A	267	10.7	12.5	57.8
			B	268	18.9	21.9	56.7
2	2′-OCH_3	2″-OCH_3	A	297	4.9	17.6	63.7
			B	304	6.8	32.3	63.7
	3′-*H*	3″-*H*	B	287	13.1	9.5	62.9
	6′-*H*	6″-*H*	A	317	71.6	122.0	63.0
			B	328	126.8	210.0	63.8
	C-1′	*C*-1″	A	302	5.6	33.8	63.2
			B	311	2.6	65.1	63.4
	C-3′	*C*-3″	A	312	31.0	69.1	63.5
			B	321	56.0	129.8	63.7
	C-4′	*C*-4″	A	303	39.0	40.8	62.9
			B	309	65.7	66.8	62.9
	C-5′	*C*-5″	A	294	40.4	15.5	63.3
			B	295	64.7	23.0	62.6

[a] For numbering of the individual positions see Fig. 1; ′ denotes positions in the aryl ring *syn*, ″ those in the aryl ring *anti* to the O—H··· N bridge.
[b] Spectra were recorded at two different field strengths: A, 7.04 T (nominal ^1H frequency 300 MHz) and B, 11.74 T (500 MHz ^1H); for further details, see Experimental.
[c] Separation $\Delta\nu$ (Hz) between the individual *syn–anti* signal pairs at the lowest temperature attainable in $CDCl_3$.
[d] Hypothetical separation $\Delta\nu$ (Hz) at the point of coalescence, extrapolated by linear regression analysis from the respective $\Delta\nu$–T correlation (see text).

tively. Among these are the ^1H signals for the *p*-CH_3 groups and for the *o*-protons 6′/6″. For the two *meta* positions, 3′/3″-H and 5′/5″-H, the proton signals have already coalesced at the lowest temperature attainable in $CDCl_3$. (Measurements in CD_2Cl_2 and in other solvents will be part of further investigations for this series of compounds.) One of the *meta* ^{13}C signals (C-5′/5″), however, clearly displays coalescence at both field strengths, as do the *ipso* positions C-1′/C-1″. For all other ^{13}C signals, *syn* and *anti* line positions are so far separated at the point of coalescence that the line broadening due to the exchange process merges them with the background. To extract these line positions would far surpass the experimental time allotted for routine experiments (1 h for ^{13}C). For the tetramethoxy derivative **2**, however, coalescence is indeed observed for two additional carbon positions, C-3′/C-3″ (*meta*) and C-4′/C-4″ (*para*, see Table 1). Coalescence temperatures T_C were determined for five positions in **1** and for seven positions in **2**, all except one at both field strengths available, spanning a range of 30° for **1**, and of 40° for **2**.

At each coalescence point, the rate constant of the chemical exchange can be derived from the Gutowsky–Holm relationship[3,11]:

$$k_C = \pi\,\Delta\nu/\sqrt{2} \qquad (1)$$

and thence, by the Eyring equation[12]

$$k = k_b\,T/h\,\exp(-\Delta G^{\ddagger}/RT) \qquad (2)$$

the free energy of activation for the exchange process, $\Delta G_C^{\ddagger}$ (see Table 1). If rotation barriers for the intramolecular reorientation of *different* triazines are to be directly compared, however, the activation parameters $\Delta H^{\ddagger}$ and $\Delta S^{\ddagger}$ are required. This is accomplished, preferentially, by complete lineshape analysis of the signal under exchange at various temperatures [13] in the proximity of the coalescence point. With the rate constants k_T of the exchange process thus determined, the activation energy then is derived from an Arrhenius plot according to the Arrhenius equation[12]

$$k = A\,\exp(-E_a/RT) \qquad (3)$$

It has already been pointed out[12] that these activation parameters might be obtained directly if coalescence could be observed for the same process at different temperatures. This was achieved for the first time by Gutowsky and Cheng,[14] who determined the *syn/anti-N*-CH_3 proton signal coalescence in dimethylformamide, -acetamide and -propionamide at three different field strengths. In a footnote to this paper, the possibility is also mentioned of extending the data set by including also ^{13}C coalescence phenomena; at the time, this was experimentally not yet feasible.

Now that a whole series of $\Delta G_C^{\ddagger}$ terms are available for the same dynamic process, however, together with the corresponding T_C values, it appeared intriguing to plot $\Delta G_C^{\ddagger}$ directly against T_C according to Gibbs–Helmholtz:[15]

$$\Delta G^{\ddagger} = \Delta H^{\ddagger} - T\,\Delta S^{\ddagger} \quad (4)$$

$$\Delta H^{\ddagger} = E_a - RT \quad (5)[16]$$

Figure 4(a) shows such a correlation for the individual coalescences determined for both **1** and **2**; a weighted linear regression analysis yields the activation parameters listed below, which are fully compatible with the process envisaged in Fig. 2:

	$\Delta H^{\ddagger}$ (kJ mol^{-1})	$\Delta S^{\ddagger}$ (J mol^{-1} K^{-1})
1	51 ± 6	$\sim 0\ (-20 \pm 24)$
2	58 ± 6	$\sim 0\ (-17 \pm 19)$

The divergences for the individual data points appear only if the graph is expanded tenfold [Fig. 4(b)]. The error limits, indicated graphically in Fig. 4(b) for **2**, were calculated by a progessive error analysis for all three activation parameters, based on the experimental error limits in determining T and $\Delta\nu$.[17] With a slope close to zero, the regression coefficient r is no longer a valid criterion for the quality of the correlation; Fig. 4(b) shows, however, that the correlation straight line lies well within the error limits for the individual data points. This likewise holds for **1**.

Coalescence data generally are evaluated in terms of Eqns (1) and (2).[12,14] With a full k_C–T_C data set available, however, one might as well directly plot the individual ln k_C *vs.* the respective $1/T_C$ values. The corresponding Arrhenius plot yields the activation energy E_a and thence, with the RT correction according to Eqn (5), once more $\Delta H^{\ddagger}$. The $\Delta H^{\ddagger}$ values for the two different evaluation procedures, not unexpectedly, are identical (see above). Since the k_C *vs.* $1/T_C$ correlation has a marked (negative) slope, however, the regression coefficient r can now be used to demonstrate the quality of the correlation. The error, given below for E_a and $\Delta H^{\ddagger}$, comes directly from the linear regression and is not derived by progressive error analysis:

	E_a (kJ mol^{-1})	r	$\Delta H^{\ddagger}$ (kJ mol^{-1})
1	53 ± 1	0.988	51 ± 1
2	61 ± 1	0.989	58 ± 1

For deriving the rate constant k_C by Eqn (1), the separation $\Delta\nu_C$ values of the respective signals at the coalescence temperature T_C are required, apart from this temperature itself. Since $\Delta\nu_C$ is not accessible by definition, a $\Delta\nu$ value is used as a rule which is determined at the slow-exchange limit, i.e. at low temperature. This procedure completely neglects, however, the fact that the chemical shifts for the positions, affected by the exchange process, may not only be temperature dependent, but also exhibit strongly divergent temperature dependences with even different signs. Katritzky *et al.*[18] have also stressed this point in a recent paper which likewise deals with the intramolecular dynamics of 1,3,5-triazines.

The $\Delta\nu$–T correlations in Fig. 5 demonstrate how strongly and differently the chemical shift difference may vary with temperature even for individual positions within one molecule. For the two ^{13}C separations given in Fig. 5, $\Delta\nu$(C-1′/1″) and $\Delta\nu$(C-5′/5″), the temperature

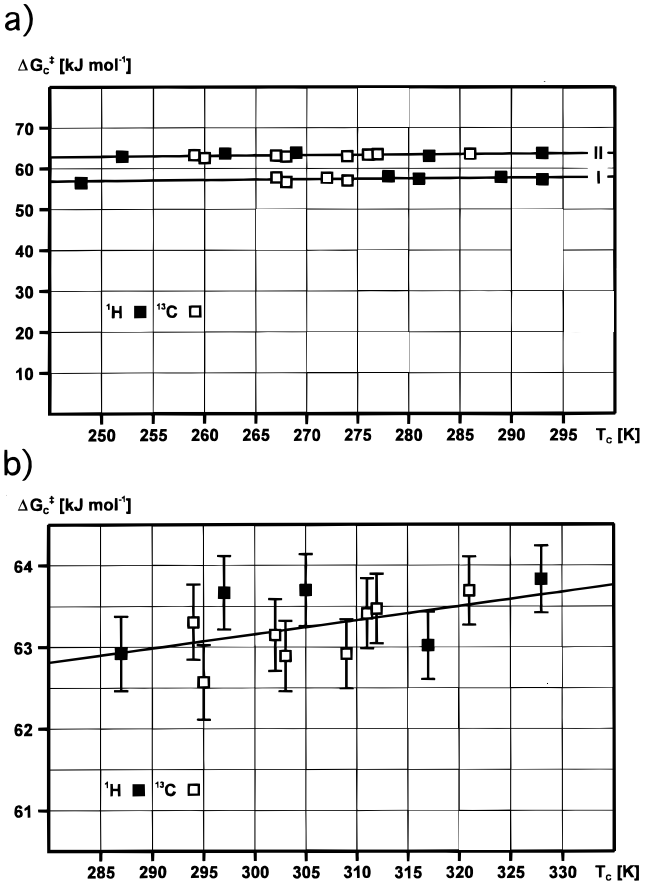

Figure 4. (a) Gibbs–Helmholtz plot for the individual $\Delta G_C^{\ddagger}$–T_C data points (see Table 1), determined for **1** and **2**. (b) $\Delta G_C^{\ddagger}$–T_C correlation for **2** with the ordinate scale expanded, and error limits indicated for each data point.

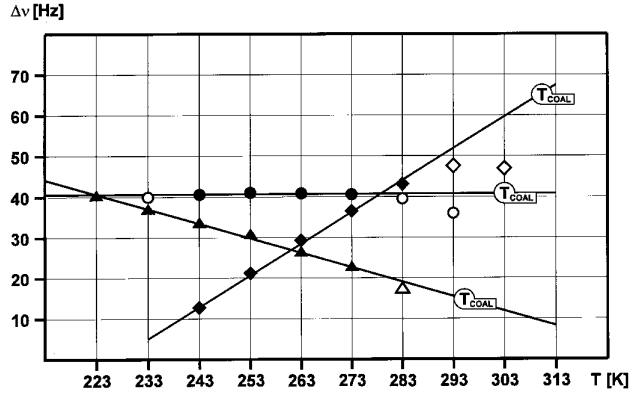

Figure 5. Temperature dependence for three *syn–anti* signal pairs in **2** (▲, C-5′/5″, 7.04 T; ◆ C-1′/1″, 11.74 T; ● C-4′/4″, 7.04 T); only those data have been included in the regression analysis where the individual signals do not yet significantly overlap (filled symbols; see text).

dependence has opposite sign; for the *para* carbon atoms C-4′/4″, in contrast, no temperature dependence becomes apparent even though these nuclei and C-5′/5″ are equidistant from the hydrogen bridge. For the reference compound **3**, without the intramolecular hydrogen bond, all ^{1}H signals uniformly show a more or less pronounced high-field shift with increasing temperature. A detailed study of more, differently substituted triazines thus might offer the possibility of actually assigning the two lines of the individual resonance pairs to the *syn* and *anti* environment.

In calculating k_C at the individual points of coalescence, and thence the $\Delta G_C^{\ddagger}$ values listed in Table 1, a $\Delta\nu$ value was employed in each case which was extrapolated by linear regression analysis from the respective $\Delta\nu$–T correlations. It is important, however, to only consider $\Delta\nu$ values for temperatures where the two lines display no interference, i.e. where there is not yet any significant overlap. As a rule, 5–8 values, determined for 10 K steps each, have been included. The error in $\Delta\nu$ is thus effectively reduced to the experimental error in determining line positions.

A lineshape analysis, performed for the coalescence of the 2′/2″-CH_3 proton signal in **1**, independently demonstrates the importance of using the proper value for the line separation $\Delta\nu$ at any given temperature. A perfect fit is obtained only with the extrapolated value for $\Delta\nu$ (see Fig. 6). Generally, the error induced by employing a slow-exchange limit value for $\Delta\nu$ is far larger than the error introduced with the temperature term. If, for instance, $\Delta G_C^{\ddagger}$ is calculated for the 2′/2″-OCH_3 proton signal coalescence at 11.74 T, employing the slow-exchange limit $\Delta\nu$ value of 6.8 Hz instead of the extrapolated value for $\Delta\nu_C$ (32.3 Hz; see Table 1, compound **2**), the free energy of activation comes out as 4 kJ mol^{-1} too high. This error in ΔG would add to the uncertainty in ΔH. A T_C value which was 'false' by 2 K, in contrast, would alter the $\Delta G_C^{\ddagger}$ value by only 0.5 kJ mol^{-1}.

For the 2′/2″-CH_3 proton signal in compound **1**, the rate of exchange k_T was determined at various temperatures by complete lineshape analysis employing, of course, the requisite $\Delta\nu$ value for each temperature. The enthalpy of activation, $\Delta H^{\ddagger}$, is thence derived as 47 kJ mol^{-1}, in good agreement with the 51 $\pm$ 6 kJ mol^{-1} from both k_C–T_C correlations.

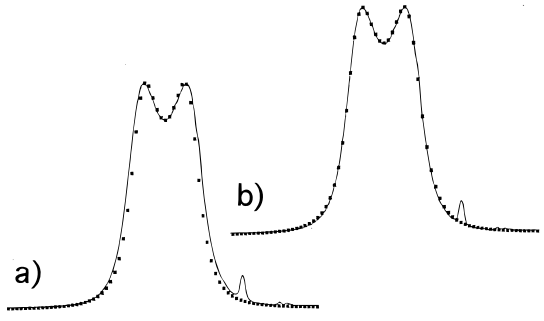

Figure 6. Lineshape of the 2′/2″-CH_3 proton signal at 276 K and 7.04 T: the solid lines represent the experimental signal and the points the best fit for the calculated lineshape with (a) the slow-exchange limit value for $\Delta\nu$ = 30.6 Hz and (b) the extrapolated value for $\Delta\nu$ = 33.2 Hz used for the calculation (see text).

CONCLUSION

The energy of activation for breaking the intramolecular hydrogen bond in the 6-(2-hydroxyaryl)-1,3,5-triazines can be directly compared with the energy of formation for the intermolecular hydrogen bond between an aza-nitrogen, incorporated in an aromatic ring, and a phenolic OH function for the system pyrimidine–phenol in carbon tetrachloride.[19] The strength of this intermolecular hydrogen bridge has been characterized as follows (with the enthalpy of formation of course with a negative sign): pyrimidine–phenol–CCl_4, $\Delta H = -22.6 \pm 2.1$ kJ mol^{-1} and $\Delta S = -58 \pm 7$ J mol^{-1} K^{-1}. The intramolecular hydrogen bond investigated here was found to be almost three times as strong. This represents direct proof of the chelate character of the hydrogen bridge in these triazines, and also explains the importance of this bond for the radiationless deactivation of photoexcited states if such triazines are employed as photostabilizers.[7,8] Since the entropy of activation, not unexpectedly, was determined as virtually zero, free energies of activation, $\Delta G^{\ddagger}$, for different triazines may now be compared directly.

As demonstrated above, a series of spectral traces at e.g. 10° intervals is a prerequisite for *any* DNMR experiment in order to obtain correct values for the signal separation $\Delta\nu$ at any given temperature. With such a 10° grid, pinpointing a specific coalescence temperature will need at least three, at most five, additional measurements with a 1° interval each. Proper lineshape analysis should likewise be based on at least five spectral traces at different temperatures around the coalescence point. The $\Delta G_C^{\ddagger}$ *vs.* T_C correlation, presented in this paper requires a minimum of four or five coalescence data sets. With a system, however, which presents a number of exchanging sites such as the triazines investigated here, one can spread these coalescence data sets over as wide a temperature range as possible, and thus gain reliability for the activation parameters.

Overall, we believe that roughly twice as many NMR measurements are necessary in this approach as for lineshape analysis. This has to be set off against the time required for fitting the individual spectral traces by optimizing each k_T.

EXPERIMENTAL

Compounds **1–3** were kindly provided by Ciba SC Recherche (Marly, Switzerland) (see also Refs 8 and 10). ^{1}H and ^{13}C NMR spectra were recorded on Bruker ARX-300 and ARX-500 spectrometers (7.04 and 11.74 T, respectively) for 0.1 M solutions in $CDCl_3$ (0.1% TMS as internal standard). For the individual measurements at a given temperature, the following standard parameters were used: ^{1}H, nominal frequency 300.13/500.13 MHz, pulse width (90°) 10.6/11.3 μs, 32K FID, digital resolution $\pm$0.16 Hz per point; ^{13}C, nominal frequency 75.48/125.77 MHz, pulse width (90°) 11.5/10.8 μs, 64K

FID, digital resolution ± 0.32 Hz per point. A 30° flip angle was employed for the individual measurements. Temperature was adjusted and controlled by a Bruker BVT-2000 variable-temperature unit which was calibrated according to van Geet.[20] To ensure maximum homogeneity after changing the temperature setting, the sample was held for 20 min at this temperature in the probehead before aquisition was started. Complete lineshape analysis was performed with an in-house program based on the Bloch equations. Error analyses, by standard statistical methods, were based on the assumptions that (a) the point of coalescence can be visually fixed to ± 1 K and (b) the error in determining the actual temperature in the probehead by the BVT-2000 unit likewise does not exceed ± 1 K.

Acknowledgements

We are grateful to Professor Dr H. E. A. Kramer for many stimulating discussions; he first introduced us to the problem of intramolecular hydrogen bridging in the (2-hydroxyaryl)-1,3,5-triazines. Special thanks are due to Drs G. Rytz and J. L. Birbaum of Ciba SC Recherche (Marly, Switzerland) for providing the triazine samples and for many helpful comments.

REFERENCES

1. J. Sandström, *Dynamic NMR Spectroscopy*. Academic Press, New York (1982).
2. L. M. Jackman and F. A. Cotton (Eds), *Dynamic NMR Spectroscopy*. Academic Press, New York (1975).
3. H. S. Gutowsky and C. H. Holm, *J. Chem. Phys.* **25**, 1228 (1956).
4. W. E. Stewart and T.H. Siddall, III, *Chem. Rev.* **70**, 517 (1970).
5. L. M. Jackman and F. A. Cotton (Eds), *Dynamic NMR Spectroscopy*, p. 204. Academic Press, New York (1982).
6. H. G. Bonacorso, M. S. B. Caro, N. Zanatta and M. A. P. Martins, *Magn. Reson. Chem.* **31**, 451 (1993).
7. H. E. A. Kramer, *GIT Labor-Fachz.* **40**, 1220 (1996); G. Rytz, J. L. Birbaum and A. Steinmann, *Chimia* **48**, 422 (1994).
8. G. J. Stueber, M. Kieninger, H. Schettler, W.Busch, B. Goeller, J. Franke, H. E. A. Kramer, H. Hoier, S. Henkel, P. Fischer, H. Port, T. Hirsch, G. Rytz and J. L. Birbaum, *J. Phys. Chem.* **99**, 10097 (1995).
9. J. Keck, H. E. A. Kramer, H. Port, T. Hirsch, P. Fischer and G. Rytz, *J. Phys. Chem.* **100**, 14468 (1996).
10. G. Stueber, *Doctoral Thesis*, Universität Stuttgart (1994).
11. J. Sandström, *Dynamic NMR Spectroscopy*, p. 1. Academic Press, New York (1982).
12. J. Sandström, Dynamic NMR Spectroscopy, p. 93. Academic Press, New York (1982).
13. G. Binsch, in *Dynamic NMR Spectroscopy*, edited by L. M. Jackman and F. A. Cotton, p. 45. Academic Press, New York (1975).
14. H. S. Gutowsky and H. N. Cheng, *J. Chem. Phys.* **63**, 2439 (1975).
15. P. W. Atkins, *Physical Chemistry*, 2nd ed., p. 165. Oxford University Press, Oxford (1982).
16. P. W. Atkins, *Physical Chemistry*, 2nd ed., p. 986. Oxford University Press, Oxford (1982).
17. A. Fettig, *Diplomarbeit*, Universität Stuttgart (1996).
18. A. R. Katritzky, I. Ghiviriga, P. J. Steel and D. C. Oniciu, *J. Chem. Soc., Perkin Trans. 2*, 443 (1996).
19. M. D. Joesten and L. J. Schaad, *Hydrogen Bonding*, p. 313. Marcel Decker, New York (1974).
20. A. L. van Geet, *Anal. Chem.* **42**, 679 (1970).

